Abelian integrals, algebraic functions and compact Riemann surfaces in the semiclassical theory of non-adiabatic collisions



1996 J. Phys. A: Math. Gen. 29 1055

(http://iopscience.iop.org/0305-4470/29/5/019)

J. Phys. A: Math. Gen. **29** (1996) 1055–1074. Printed in the UK

# Abelian integrals, algebraic functions and compact Riemann surfaces in the semiclassical theory of non-adiabatic collisions

Kai-Shue Lam

Physics Department, California State Polytechnic University, Pomona, CA 91768, USA

Received 3 January 1995, in final form 24 October 1995

**Abstract.** Some beautiful classical results in the mathematics of Abelian integrals, algebraic functions and compact Riemann surfaces, which are relatively little used in physics applications (except in string theory), are shown to be relevant in the semiclassical theory of non-adiabatic collisions. These results are discussed in the context of the adiabatic theorem for the time-dependent Schrödinger equation describing multi-(electronic) level molecular collision systems. It is found that the different potential energy surfaces governing nuclear motion can be regarded as a single algebraic function $\varepsilon(t)$ of the complex time variable $t$. The topological and analytic properties of the compact Riemann $t$-surface for this algebraic function then determine the nature of the non-adiabatic quantum transitions. The amplitudes of these transitions are given by a generalization of Dykhne's formula, whose main feature is an Abelian (action) integral of the Abelian differential $\varepsilon(t)\,\mathrm{d}t$. These ideas are applied to a rederivation of the Landau–Zener formula, which is shown to result from a model with a genus zero Riemann surface. A genus one model, illustrating more substantially the interplay between topology, analyticity and quantum transitions, is also discussed in detail.

## 1. Introduction

The semiclassical theory of collisional dynamics has a long and interesting history, reaching back to the early days of quantum mechanics [1]. During its initial phase it was regarded mainly as an approximation scheme to quantum mechanics, albeit a scheme with great intuitive appeal (that of classical mechanics) and practical applicability. The situation changed somewhat when it was realized, over two decades ago, that this theory can be cast in the language of Feynman path integrals [2, 3], and that classical trajectories can be continued analytically into either the complex time or coordinate domain to yield quantum mechanical results [4]. From then on, semiclassical methodology acquired a more independent status and was developed more as a theoretical framework in its own right, while its applications in diverse fields of physics continued to grow [5]. More recently two important developments in theoretical physics have brought semiclassical theories very much to the fore. The first is the intense interest in the relationship between classical and quantum chaos in various dynamical systems and, more generally, in a deeper understanding of the relationship between classical and quantum mechanics [6]. The second is Berry's discovery [7, 8] of the universal presence of non-dynamical (geometrical) phases in the evolution of systems separable into 'fast' and 'slow' degrees of freedom, traditionally the prime focus of study by semiclassical techniques. These developments have not only yielded deep and unifying ideas in physics [6, 8] but also revealed the great utility of a host of mathematical

0305-4470/96/051055+20$19.50  

techniques. In particular topological and geometrical methods have assumed great relevance in many problems of collisional dynamics [8, 9].

In this work we examine afresh the problem of non-perturbative solutions to the time-dependent Schrödinger equation describing non-adiabatic transitions in a multi-level system. We hope to demonstrate that certain well established, beautiful, but relatively little used, results in classical function theory and algebraic geometry provide a remarkably natural and appealing framework for the description of the physics of non-adiabatic transitions. In our opinion, this framework also promises to yield calculational advantages as well as deeper insights into the nature of semiclassical mechanics.

Our problem traces back to the well known Landau–Zener formula for non-adiabatic transitions [10, 11]. Landau first exploited, within the framework of the JWKB approximation, the technique of calculating the classical action to yield a quantum mechanical transition amplitude by complexification of the nuclear coordinate variable. Dykhne [12] later generalized this method to obtain a non-perturbative solution to the time-dependent Schrödinger equation in the form of an energy contour integral over time treated as a complex variable. Pechukas [2], Miller [3, 4] and Miller and George [4] then succeeded in formulating semiclassical dynamics (classical mechanics plus quantum superposition) in terms of Feynman path integrals and studied extensively the technique of time or coordinate complexification. Hwang and Pechukas [13] also attempted to justify the Miller–George theory by proving the existence of adiabatic contours in the complex time plane corresponding to non-adiabatic transitions along the real time axis. The significance of the Landau–Zener and Dykhne formulae and the Hwang–Pechukas adiabatic theorem beyond their immediate applicability was recently underscored by Moody *et al* [14] in the context of geometric phases in the complex time plane.

Although this large body of work was aimed chiefly at producing concrete and computationally useful results, it opens up many exciting avenues of exploration in the underlying mathematics. We will focus on the following situation. Let $H_{el}(R; r)$ be the electronic Hamiltonian in a molecular collision problem parametrized by the nuclear coordinates $R_1, \ldots, R_m$ ($R$ and $r$ denote, collectively, the nuclear and electronic coordinates, respectively). We assume that there exists a finite $N$-dimensional subspace of the Hilbert space of electronic states that is invariant with respect to $H_{el}(R; r)$. The adiabatic potential energy surfaces for nuclear motion, $\varepsilon_n(R)$, satisfying the Schrödinger equation

$$H_{el}(R; r)\phi_n(R; r) = \varepsilon_n(R)\phi_n(R; r)$$

can then be obtained by solving a polynomial equation (in $\varepsilon$) of the form

$$\varepsilon^N + \alpha_1(R)\varepsilon^{N-1} + \cdots + \alpha_N(R) = 0$$

in which $\alpha_i(R)$ are functions of the matrix elements of $H_{el}$ in an arbitrary representation. This polynomial equation defines a complex analytic variety $\mathbb{V}$ in $\mathbb{C}^{m+1}$. If we further assume the existence of classical trajectories for nuclear motion, then each of the nuclear coordinates $R_i$ becomes a function of the time variable $t$. These functions, when analytically continued, can be regarded as single-valued meromorphic functions of the complex-valued time variable. The time variable serves to parametrize a curve in $\mathbb{V}$ defined by

$$\varepsilon^N + a_1(t)\varepsilon^{N-1} + \cdots + a_N(t) = 0$$

where $a_i(t) \equiv \alpha_i(R(t))$. In the case of only one nuclear coordinate ($m = 1$) the nuclear trajectory $R(t)$ and $\varepsilon(t)$ (defined by the above equation) actually furnish a uniformization of $\mathbb{V}$. In the more general case ($m > 1$), we can still use the function $\varepsilon(t) \equiv \varepsilon(\alpha_i(R_j(t)))$ to impose a complex structure on the curve parametrized by $t$, and thus obtain the corresponding Riemann surface of $\varepsilon(t)$. The main question is then the following. When

classical mechanics is analytically continued in the above sense, how do the topological and complex structures of the resulting Riemann surface affect the dynamics of a system described semiclassically by the Schrödinger equation? We will approach this problem from the viewpoint of a physicist, and address this work mainly to physicists who, like the author, may not be entirely at home with the theory of Riemann surfaces and algebraic curves. Our discussion on the relevant mathematics will thus be quite elementary and largely non-technical.

We begin by showing how the different branches of an algebraic function may correspond precisely to the different potential energy curves in a multi-level problem. Next we relate the analytic properties of this function to the genus of its Riemann surface by the Riemann–Hurwitz formula [15] (section 2). A generalization of Dykhne's formula is then proposed with the help of the Hwang–Pechukas adiabatic theorem in the complex plane (section 3). In section 4 we demonstrate the power and elegance of the Riemann surface approach by providing yet another derivation of the Landau–Zener formula—an entirely function theoretic one that highlights the crucial roles played by topology and analyticity. We will see that the model on which this formula is based leads to a genus zero Riemann surface—topologically a 2-sphere, with trivial fundamental group (all closed loops deformable to a point). This topological feature is the deciding factor contributing to the simplicity of the formula (equation (27)). Section 5 pursues a simple model leading to a genus one Riemann surface—topologically a 2-torus. This slight complication in topology, together with a corresponding complication in the analytic properties of the Abelian action differential, lead to an interesting but much more complicated counterpart of the Landau–Zener formula, involving the fundamental periods of elliptic functions. Our discussion of the genus one model also makes contact with the Riemann–Roch theorem [16], a powerful, classical theorem relating the analytic properties of meromorphic functions and Abelian differentials on a Riemann surface to the topology of the surface. Finally, section 6 is devoted to some speculations on the directions for further study.

## 2. Quantum transitions as manifestations of topology and analyticity

We assume that the time-dependent Schrödinger equation

$$H(t)\Psi(t) = \mathrm{i}\hbar\frac{\partial\Psi}{\partial t} \tag{1}$$

describes the time evolution of non-degenerate electronic states in a molecular collision system. The Hamiltonian $H(t)$ depends on time implicitly through a choice of nuclear trajectories $R(t)$. The instantaneous eigenfunctions $\phi(t)$ of $H(t)$ satisfying

$$H(t)\phi_n(t) = \varepsilon_n(t)\phi_n(t) \tag{2}$$

are assumed to form a complete orthonormal set, where $\varepsilon_n(t)$, for real $t$, is the potential energy curve governing nuclear motion on the $n$th electronic level in the adiabatic (diagonal) representation. Non-degeneracy means that $\varepsilon_i(t) \neq \varepsilon_j(t)$ for all real $t$, and $i \neq j$. For molecular collision problems, one usually works with a finite-dimensional subspace of the Hilbert space generated by $\{\phi_n\}$ that is invariant under $H$. For an $N$-level problem, and in an arbitrary representation $\{\theta_n(t)\}$, the $N \times N$ hermitian matrix representing $H(t)$ is not necessarily diagonal, and the $\varepsilon_n(t)$ are obtained from diagonalization, i.e. solutions of the characteristic equation

$$\det|H_{ij}(t) - \varepsilon| = 0 \tag{3}$$

where

$$H_{ij}(t) \equiv \langle \theta_i | H | \theta_j \rangle.$$

Equation (3) is in general a polynomial equation of the form

$$\varepsilon^N + a_1(t)\varepsilon^{N-1} + \cdots + a_N(t) = 0 \tag{4}$$

where the coefficients $a_i(t)$ are functions of $H_{ij}(t)$. This equation defines an affine analytic curve in $\mathbb{C}^2$.

For fixed real $t$, non-degeneracy and the fundamental theorem of algebra imply that there are $N$ distinct real roots—the eigenvalues $\varepsilon_i(t)$, $i = 1, 2, \ldots, N$. However, and this is the crucial point, there always exist complex values of $t$ for which equation (4) has repeated roots. These complex $t$ values are the branch points of the multivalued function $\varepsilon(t)$ determined by equation (4). $\varepsilon(t)$ can be made single valued by considering its domain as an $N$-sheeted Riemann surface $M$ (instead of the complex plane $\mathbb{C}$) whose sheets are joined together at the branch points and along cuts. The details of how these cuts are made do not affect the topology of the surface. What is important for our physical application is that the topology dictates the possible non-homotopic smooth paths on $M$ (those not continuously deformable into each other) along which $\varepsilon(t)$ varies from eigenvalue of $H$ to another. Distinct, non-intersecting, potential energy curves $\varepsilon_i(t)$ considered as $N$ real functions of real $t$, in fact, when analytically continued, constitute a single potential energy meromorphic function $\varepsilon(t) : M \to \mathbb{C}U\{\infty\}$, where $M$ is a Riemann surface, i.e. a one-dimensional connected complex manifold.

Thus the dynamics of a multi-level system can conveniently be viewed as dynamics on a Riemann surface whose topological and complex structures determine the nature of quantum transitions. We will see (in the examples discussed in sections 4 and 5) that such topological properties as the genus, the fundamental group $\Pi_1(M)$ and the first homology group $H_1(M)$, as well as such analytical properties as the degree of $\varepsilon(t)$ (the number of branches), and the singularities and residues of the Abelian differential $\varepsilon(t)\,\mathrm{d}t$, all play very important roles.

It is a remarkable theorem [17] in classical function theory that if the coefficients $a_i(t)$ in equation (4) are rational functions of $t$, then the Riemann surface of $\varepsilon(t)$ is compact (homeomorphic to a sphere with $g$ handles, $g = 0, 1, 2, \ldots$ being the genus of the surface). Under the conditions of this theorem, equation (4) defines an algebraic curve [16] and the meromorphic function $\varepsilon(t)$ is an example of an algebraic function [17]. The converse of this theorem is also true: any compact Riemann surface is conformally equivalent to the Riemann surface of some algebraic function. The simple topology of compact Riemann surfaces allows a relatively straightforward identification of the paths leading to quantum transitions based on $\Pi_1(M) = \mathbb{Z}^{2g}$ for a surface of genus $g$, as well as relatively simple calculations of the corresponding action integrals based on $H_1(M)$. This will be discussed further in the next section and demonstrated in some detail for the genus one example in section 5.

The genus $g$ of the Riemann surface of the algebraic function $\varepsilon(t)$ can be easily determined by another remarkable theorem for compact Riemann surfaces—the Riemann–Hurwitz formula [17]—which relates $g$ to the number of branch points $(B)$, and the degree $(N)$, of $\varepsilon(t)$. Specifically

$$g = B/2 - N + 1. \tag{5}$$

This formula immediately implies that the number of branch points must be even. Its simple and straightforward utility will again be illustrated in the examples in sections 4 and 5.

Of course there is no *a priori* reason why the coefficients $a_i(t)$ in equation (4) should be rational functions of $t$ and, in fact, in many semiclassical model studies [1], they are not. Rational functions, however, can in practice be used to approximate any smooth function locally to any desired degree of accuracy. As will be seen below, the Landau–Zener model is based on approximating potential curves locally (near the crossing point) by the simplest possible non-trivial rational functions of $t$ (linear functions). The success and importance of this model has motivated us to exploit the convenient properties of compact Riemann surfaces in our investigation. Thus, in this work, we will confine our attention to models of the Hamiltonian $H(t)$ leading to such surfaces.

## 3. The adiabatic theorem and Abelian integrals in the transition amplitude

The adiabatic theorem on the real time $(t)$ axis states that for a non-degenerate, slowly varying, time-dependent Hamiltonian $H(t)$ the solution $\Psi(t)$ of the Schrödinger equation (1) with $\Psi(0) = \phi_n(0)$ (cf equation (2)) is

$$\Psi(t) = \phi_n(t) \exp\left\{ \mathrm{i}\gamma_n(t) - \frac{\mathrm{i}}{\bar{h}} \int_0^t \varepsilon_n(t)\, \mathrm{d}t \right\} \tag{6}$$

in the semiclassical limit $\bar{h} \to 0$. The quantity

$$\gamma_n(t) \equiv \mathrm{i} \int_0^t \langle \phi_n | \dot{\phi}_n \rangle \, \mathrm{d}t \tag{7}$$

is the so-called geometric (Berry) phase, which can be shown quite generally to be real provided $\{\phi_n(t)\}$ is an orthonormal set for all $t$.

The condition of adiabaticity (slow time variation of $H(t)$) amounts to the limit $T \to \infty$, where $T$ is the time interval over which $H(t)$ changes significantly. As pointed out by Hwang and Pechukas [13], there is a close connection between the adiabatic limit and the classical limit $\bar{h} \to 0$. The correspondence between these two limits is usually achieved by the time-scaling $\tau = t/T$, which leads to the time-scaled Schrödinger equation

$$\mathrm{i}\bar{h}' \frac{\partial \Psi'}{\partial \tau} = H'(\tau)\Psi'(\tau)$$

where $\bar{h}' \equiv \bar{h}/T$, $H'(\tau) \equiv H(T\tau)$, and $\Psi'(\tau) \equiv \Psi(T\tau)$. However, Berry [18] also pointed out that the two limits are not in general equivalent, since $H'(\tau)$ in the above equation may have a concealed $\bar{h}$-dependence. Thus the classical limit $\bar{h} \to 0$ (on both sides of the Schrödinger equation) and $T =$ constant may not be equivalent to the limit $T \to \infty$ while keeping $\bar{h}$ constant.

To restore the equivalence, we make a distinction between the classical limit ($\bar{h} \to 0$ on both sides of the Schrödinger equation (1)) and the semiclassical limit ($\bar{h} \to 0$ on only the right-hand side of equation (1)). This distinction is justified in the present context since $H(t)$ is presumably determined from a quantum mechanical treatment of the electronic motion, where $\bar{h} \neq 0$ strictly. In the semiclassical limit the parameters $a, b, c$ in our model Hamiltonians (equations (18) and (28)) are strictly constants (even though they may involve $\bar{h}$ in principle), and are not affected by the limit $\bar{h} \to 0$. The equivalence between the adiabatic and the semiclassical limits is borne out by the Landau–Zener formula (equation (27)), in which $a \propto 1/T$ and $b =$ constant.

Hwang and Pechukas [13] also generalized the adiabatic theorem from the real axis to the complex plane $\mathbb{C}$ to incorporate quantum transitions from state $i$ to state $j$. This result can be restated in terms of the $t$-Riemann surface: if the energy function $\varepsilon(t)$ is viewed as a function on the Riemann surface $M$, $\varepsilon(t) : M \to \mathbb{C} \cup \{\infty\}$, specified by equation (4),

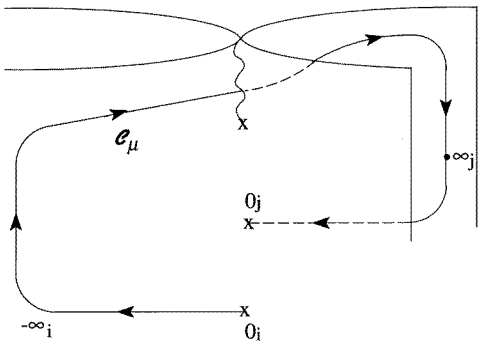


**Figure 1.** A contour $\mathcal{C}_\mu$ from the point $t = 0$ on the real axis of the $i$th Riemann sheet ($0_i$) to the point $t = 0$ on the real axis of the $j$th Riemann sheet ($0_j$) along which the adiabatic theorem holds. The contour leads to a quantum transition from state $i$ to state $j$. In the general case sheets $i$ and $j$ may not be connected directly.

then there exists a contour $\mathcal{C}$ on $M$ leading from the $i$th sheet to the $j$th sheet such that equation (6) holds along $\mathcal{C}$ in the semiclassical limit $\overline{h} \to 0$. Figure 1 illustrates one such contour $\mathcal{C}_\mu$. ($\mu$ is a homology index, as explained below.) The adiabatic theorem thus implies that, along $\mathcal{C}$, the solution to the Schrödinger equation (1) describing a system initially in state $i$ is given by

$$\Psi_{\mathcal{C}}(t) = \phi_{\mathcal{C}}(t) \exp\left\{ \mathrm{i}\gamma_{\mathcal{C}}(t) - \frac{\mathrm{i}}{\overline{h}} \int_{0_i(\mathcal{C})}^{t} \varepsilon(t)\, \mathrm{d}t \right\} \tag{8}$$

where $\phi_{\mathcal{C}}(t)$ is the analytic continuation of $\phi_i(t)$ from the real time axis (on the $i$th sheet of $M$) to other regions of $M$ along $\mathcal{C}$. The geometric phase $\gamma_{\mathcal{C}}(t)$ in equation (8) is given by

$$\gamma_{\mathcal{C}}(t) = \mathrm{i} \int_{0_i(\mathcal{C})}^{t} \mathrm{d}t \, \langle \phi_{\mathcal{C}}(t) | \dot{\phi}_{\mathcal{C}}(t) \rangle. \tag{9}$$

Now the general solution of the Schrödinger equation (1) on the real time axis is

$$\Psi(t) = \sum_{l=1}^{N} C_l(t) \phi_l(t) \exp\left\{ -\frac{\mathrm{i}}{\overline{h}} \int_0^t \varepsilon_l(t)\, \mathrm{d}t \right\}. \tag{10}$$

Equation (8) thus satisfies the boundary conditions

$$\Psi_{\mathcal{C}}(-\infty_i) = C_i(-\infty) \phi_i(-\infty) \exp\left\{ -\frac{\mathrm{i}}{\overline{h}} \int_0^{-\infty} \varepsilon_i(t)\, \mathrm{d}t \right\} \tag{11}$$

and

$$\Psi_{\mathcal{C}}(\infty_j) = C_j(\infty) \phi_j(\infty) \exp\left\{ -\frac{\mathrm{i}}{\overline{h}} \int_0^{\infty} \varepsilon_j(t)\, \mathrm{d}t \right\} \tag{12}$$

where in the above two equations all time values are real and

$$|C_i(-\infty)|^2 = 1. \tag{13}$$

The boundary condition equation (11) is equivalent to the following boundary condition on the geometric phase:

$$\exp(\mathrm{i}\gamma_{\mathcal{C}}(-\infty_i)) = C_i(-\infty) = \mathrm{e}^{\mathrm{i}\theta} \qquad (\theta \text{ real}). \tag{14}$$

Comparing equation (8) with equation (12), we have

$$\exp\{\mathrm{i}\gamma_{\mathcal{C}}(\infty_j)\}\exp\left\{-\frac{\mathrm{i}}{\hbar}\int_{0_i(\mathcal{C})}^{\infty_j}\varepsilon(t)\,\mathrm{d}t\right\} = C_j(\infty_j)\exp\left\{-\frac{\mathrm{i}}{\hbar}\int_{0_j}^{\infty_j}\varepsilon(t)\,\mathrm{d}t\right\}. \tag{15}$$

Thus for a path $\mathcal{C}$ from $0_i$ to $0_j$ on which the adiabatic theorem holds, the transition amplitude from state $i$ to state $j$ is given by

$$C_j(\infty_j) = \exp\{\mathrm{i}\gamma_{\mathcal{C}}(\infty_j)\}\exp\left\{-\frac{\mathrm{i}}{\hbar}\int_{\mathcal{C}}\varepsilon(t)\,\mathrm{d}t\right\}. \tag{16}$$

The adiabatic theorem also necessarily implies that the path $\mathcal{C}(0_i \to 0_j)$ is one where the Abelian integral

$$\int_{\mathcal{C}}\varepsilon(t)\,\mathrm{d}t$$

has a negative imaginary part, to insure that as $\hbar \to 0$ the transition probability does not increase exponentially. This requirement applies only to the entire path and not necessarily to a localized segment. Indeed, any valid $\mathcal{C}$ can be written as

$$\mathcal{C} = \mathcal{C} + \Delta\mathcal{C} - \Delta\mathcal{C}$$

where $\Delta\mathcal{C}$ is a localized segment on which the above Abelian integral has a positive imaginary part.

In general there may be several non-homotopic paths $\mathcal{C}_\lambda$ in $M$ from $0_i$ to $0_j$ satisfying the adiabatic theorem, where $\lambda$ is a homotopy index. Consider $\lambda_1 \neq \lambda_2$ such that $\mathcal{C}_{\lambda_1}$ and $\mathcal{C}_{\lambda_2}$ correspond to the same path ($\mathcal{C}_{\lambda_1}$ and $\mathcal{C}_{\lambda_2}$ may consist of non-commuting loops traversed in different orders). One still has

$$\int_{\mathcal{C}_{\lambda_1}}\varepsilon(t)\,\mathrm{d}t = \int_{\mathcal{C}_{\lambda_2}}\varepsilon(t)\,\mathrm{d}t$$

or

$$\int_{\mathcal{C}_{\lambda_1}\mathcal{C}_{\lambda_2}^{-1}}\varepsilon(t)\,\mathrm{d}t = 0.$$

Now $f(\mathcal{C}_\lambda) = \int_{\mathcal{C}_\lambda}\varepsilon(t)\,\mathrm{d}t$ considered as a map $f{:}\Pi_1(M) \to \mathbb{C}$ is a group homomorphism provided two paths $C_{\lambda k_1}$ and $C_{\lambda k_2}(k_1 \neq k_2)$ within the same homotopy class do not enclose singularities with non-zero residues of the Abelian differential $\varepsilon(t)\,\mathrm{d}t$. In this case, the fact that $\mathbb{C}$ is Abelian implies that $f$ is more appropriately considered as an injective map from $H_1(M)$ to $\mathbb{C}$, since, by a well known theorem, $H_1(M)$, the first homology group of $M$, is the Abelianization of $\Pi_1(M)$, i.e. $H_1(M) = \Pi_1(M)/[\Pi_1, \Pi_1]$, where $[\Pi_1, \Pi_1]$ is the commutator subgroup of $\Pi_1(M)$. Thus we need to label the paths leading to distinct values of the Abelian integral $\int\varepsilon(t)\,\mathrm{d}t$ by $\mathcal{C}_\mu$, where $\mu$ is a homology index, rather than a homotopy index.

Finally, to take into account the possible existence of singularities of $\varepsilon(t)\,\mathrm{d}t$ with non-zero residues, we recognize that, within each homology class $\mu$, there may be distinct paths $\mathcal{C}_{\mu k_1}$ and $\mathcal{C}_{\mu k_2}(k_1 \neq k_2)$ such that

$$\int_{\mathcal{C}_{\mu k_1}}\varepsilon(t)\,\mathrm{d}t \neq \int_{\mathcal{C}_{\mu k_2}}\varepsilon(t)\,\mathrm{d}t$$

if the loop $\mathcal{C}_{\mu k_1}\mathcal{C}_{\mu k_2}^{-1}$ encloses such singularities. The total transition amplitude is thus given by

$$C_j(\infty_j) = \sum_\mu \exp\{\mathrm{i}\gamma_{\mathcal{C}_\mu}(\infty_j)\}\sum_k \exp\left\{-\frac{\mathrm{i}}{\hbar}\int_{\mathcal{C}_{\mu k}}\varepsilon(t)\,\mathrm{d}t\right\} \tag{17}$$

where the sum over $\mu$ is over the homology classes and that over $k$ is over the paths in each homology class leading to distinct values, with negative imaginary parts, for the Abelian integral $\int \varepsilon(t)\,\mathrm{d}t$. We see that since $\gamma_{\mathcal{C}_\mu}(\infty_j)$ is real for all $\mu$, the geometric phase factor

$$\exp\{\mathrm{i}\gamma_{\mathcal{C}_\mu}(\infty_j)\}$$

gives a $U(1)$ representation of $H_1(M)$. Equation (17) displays clearly the importance of the topology of $M$ and the analytic properties of the Abelian integral $\int \varepsilon(t)\,\mathrm{d}t$ in the calculation of semiclassical transition amplitudes [19]. This equation for the transition amplitude is the generalization of Dykhne's formula that we seek. It will be the basis for our calculations in the next two sections. We note in advance that these calculations are based on examples with $g \leqslant 1$. The corresponding $\Pi_1(M)$'s are Abelian and thus $\Pi_1(M) = H_1(M)$ for these cases.

## 4. The Landau–Zener formula revisited: dynamics on a genus zero Riemann surface

The simplest model describing non-adiabatic transitions is the Landau–Zener model for a two-state problem. In this model the electronic Hamiltonian $H(t)$ is given by

$$H(t) = \begin{pmatrix} at & b \\ b & -at \end{pmatrix} \tag{18}$$

where $a$ and $b$ are positive real constants. Physically the diagonal elements represent two intersecting potential curves. Thus the quantity $a$ can be interpreted as the product of some instantaneous velocity of nuclear motion and the slope of one of the curves at the crossing point, while $b$ is the non-adiabatic coupling. The solutions of equation (3) or (4) for the adiabatic potential energy surfaces are immediately given by

$$\varepsilon(t) = \mp a\sqrt{\left(t + \mathrm{i}\frac{b}{a}\right)\left(t - \mathrm{i}\frac{b}{a}\right)}. \tag{19}$$

The algebraic function $\varepsilon(t)$ thus has two branch points (at $t = \pm \mathrm{i}b/a$) and two branches. Setting $B = 2$ and $N = 2$ in equation (5) (the Riemann–Hurwitz formula), the Riemann surface $M$ of $\varepsilon(t)$ is seen to be of genus zero ($g = 0$), or topologically a 2-sphere. This fact can also be seen very simply by the topological illustrations of figure 2, which shows one way of constructing $M$ from two distinct (cut) sheets of $\mathbb{C}$. (Other ways result from alternate ways of cutting the $t$-plane beginning and ending at the branch points $\pm \mathrm{i}b/a$. All lead to a 2-sphere for $M$.)

The Abelian differential $\varepsilon(t)\,\mathrm{d}t$, with $\varepsilon(t)$ given by equation (19), clearly has singularities only at the two distinct points at infinity: $t = \infty_1, \infty_2$ (see figure 2). The subscripts 1 and 2 refer to the Riemann sheets corresponding to the $-$ and $+$ branches in equation (19), respectively. To determine the nature of these singularities, we let $z = 1/t$ and expand around $z = 0$. Thus, letting $t_B = \mathrm{i}b/a$, we have

$$\begin{aligned} \varepsilon(t)\mathrm{d}t &= \mp\frac{a}{z^3}(1 + t_B z)^{1/2}(1 - t_B z)^{1/2}\,\mathrm{d}z \\ &= \pm\left(\frac{a}{z^3} - \frac{at_B^2}{2}\frac{1}{z} + \cdots\right)\mathrm{d}z. \end{aligned} \tag{20}$$

Hence $\infty_{1,2}$ are third-order poles of $\varepsilon(t)\,\mathrm{d}t$ with non-zero residues given by

$$\mathrm{Res}(\infty_{\frac{1}{2}}) = \mp\frac{at_B^2}{2} = \pm\frac{b^2}{2a}. \tag{21}$$

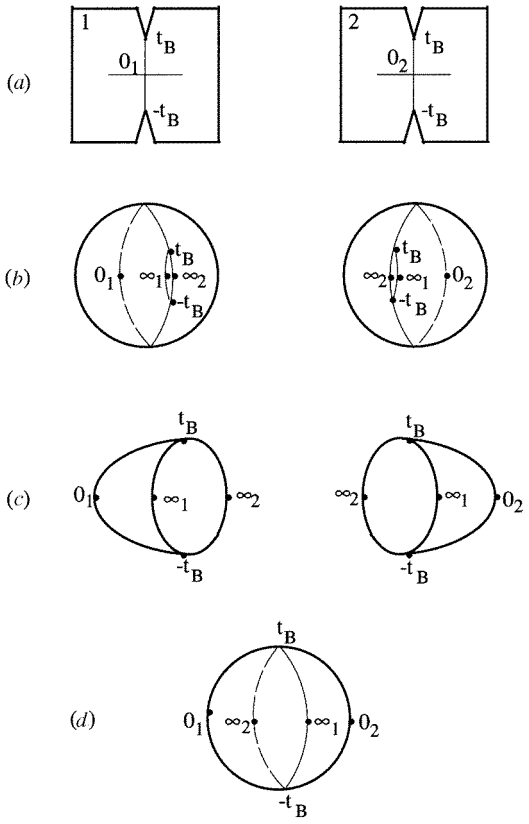


**Figure 2.** The construction of the Riemann surface $M$ (a 2-sphere) of $\varepsilon(t)$ (equation (19)) for the Landau–Zener model. One proceeds from ($a$) distinct sheets of cut $\mathbb{C}$ planes (1 and 2) with the branch points and cuts as shown ($t_B = \mathrm{i}b/a$), through 1-point compactifications to ($b$) the corresponding Riemann spheres with cuts, through homeomorphic deformations of the cut-spheres to ($c$) the corresponding hemispheres, and finally, by joining the hemispheres with matching boundaries, to ($d$) the 2-sphere. In ($a$) sheets 1, 2 correspond to the $-$ and $+$ signs in equation (19), respectively.

We note that equation (21) confirms the residue theorem: the sum of the residues of an Abelian differential on a compact Riemann surface is always zero [15].

The fundamental group $\Pi_1(M)$ for a 2-sphere [$= H_1(M)$] is trivial (consisting only of the identity element). Hence in equation (17) for the transition amplitude there is no summation over $\mu$ (the homotopy classes of $M$) and the geometric phase factor $\exp\{\mathrm{i}\gamma_{\mathcal{C}_\mu}(\infty)\}$ (being a $U(1)$ representation of $\Pi_1(M)$) can be set equal to unity. For the transition $1 \to 2$, equation (17) then reads

$$C_2(\infty_2) = \sum_k \exp\left\{-\frac{\mathrm{i}}{\hbar}\int_{\mathcal{C}_k} \varepsilon(t)\,\mathrm{d}t\right\} \tag{22}$$

where $\mathcal{C}_k$ is a path on $M$ from $0_1$ to $0_2$ (cf figures 1 and 2), and the sum over $k$ is over paths leading to distinct values (with negative imaginary parts) for the Abelian integral $\int \varepsilon(t)\,\mathrm{d}t$. (Distinct values arise because of the presence of singularities of $\varepsilon(t)\,\mathrm{d}t$ with non-zero residues.)

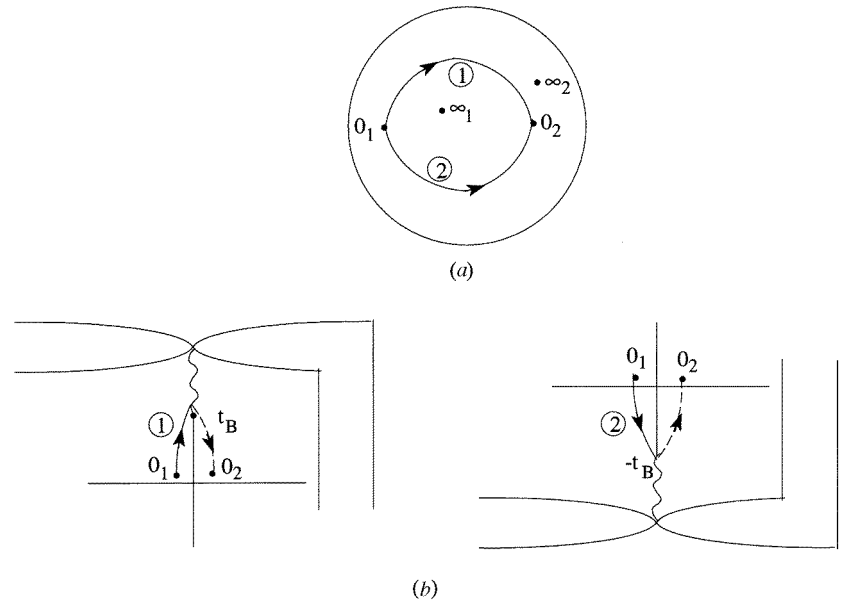


**Figure 3.** Direct paths leading to distinct values for the Abelian integral in equation (22) for the Landau–Zener model, whose Riemann surface is a sphere: (*a*) shows the paths on the sphere; (*b*) shows these paths on the corresponding Riemann sheets, deformed to run entirely along the imaginary axes.

There are two direct paths on $M$, designated 1 and 2 in figure 3(*a*), that give rise to distinct values of $\int \varepsilon(t)\,\mathrm{d}t$. These can also be represented on the Riemann sheets of $\varepsilon(t)$ (cut planes) as in figure 3(*b*), in which the contours run entirely along the imaginary axes of the sheets. Since both branches of $\varepsilon(t)$ are real on the real axis (cf equation (19)), the reflection principle on $\mathbb{C}$ implies

$$\int_{①} \varepsilon(t)\,\mathrm{d}t = \left(\int_{②} \varepsilon(t)\,\mathrm{d}t\right)^{*}. \tag{23}$$

Furthermore, we can also conclude from equation (19) that both $\int_{①}\varepsilon(t)\,\mathrm{d}t$ and $\int_{②}\varepsilon(t)\,\mathrm{d}t$ are purely imaginary. Thus on setting $\int_{①}\varepsilon(t)\,\mathrm{d}t = \mathrm{i}I$, $I$ real, the residue theorem implies that (figure 3(*a*))

$$\int_{②} \varepsilon(t)\,\mathrm{d}t - \int_{①} \varepsilon(t)\,\mathrm{d}t = -2\mathrm{i}I = 2\pi\,\mathrm{i}\,\mathrm{Res}(\infty_1) = (2\pi\,\mathrm{i})\left(\frac{b^2}{2a}\right). \tag{24}$$

According to equation (22), we have to sum over all paths $\mathcal{C}_k$ such that each $\int_{\mathcal{C}_k}\varepsilon(t)\,\mathrm{d}t$ has a negative imaginary part. Figure 3(*a*) and the value of $\mathrm{Res}(\infty_1)$ given by equation (21) show that, for a positive integer $k$, $\mathcal{C}_k$ is of the form

$$\mathcal{C}_k = ① + k \text{ clockwise loops around } \infty_1. \tag{25}$$

(The anticlockwise loops yield positive imaginary parts for the integral.)

The transition amplitude can finally be written as

$$C_2(\infty) = \exp\left(-\frac{\pi b^2}{2a\bar{h}}\right)\sum_{k=0}^{\infty}\exp\left(-\frac{\pi k b^2}{a\bar{h}}\right) = \frac{\exp(-\pi b^2/2a\bar{h})}{1-\exp(-\pi b^2/a\bar{h})}. \tag{26}$$

The leading term of the transition probability is thus

$$P_{1\to 2} \simeq \exp\left(-\frac{\pi b^2}{a\bar{h}}\right) \tag{27}$$

which is the Landau–Zener formula.

We note that $C_2(\infty)$ in equation (26) can only be interpreted as a transition amplitude if it is less than one, which is the case only when $\pi b^2/2a\bar{h}$ is larger than $\sim 0.5$ as $\bar{h} \to 0$. The Landau–Zener formula (equation (27)), however, suffers from no such limitation.

## 5. Dynamics on a genus one Riemann surface

We now consider the following Hamiltonian

$$H(t) = \begin{pmatrix} at & c \\ c & b/t \end{pmatrix} \tag{28}$$

where $a$, $b$, $c$ are positive real constants and $c^2 \neq ab$. The solutions of equation (4) for the adiabatic potential energy surfaces are given by

$$\varepsilon(t) = \left(\frac{1}{2}at + \frac{b}{t}\right) \mp \frac{a}{2t}\sqrt{(t+\sqrt{\alpha})(t-\sqrt{\alpha})(t+\sqrt{\beta})(t-\sqrt{\beta})} \tag{29}$$

where

$$\begin{matrix}\alpha \\ \beta\end{matrix} = \left(\frac{ab-2c^2}{a^2}\right) \pm \frac{2c}{a^2}\sqrt{c^2-ab}. \tag{30}$$

The algebraic function $\varepsilon(t)$ of equation (29) has two branches, and four branch points: $\pm\sqrt{\alpha}$ and $\pm\sqrt{\beta}$. The Riemann–Hurwitz formula then implies that $g = 1$ (on setting $B = 4$ and $N = 2$ in equation (5)) and thus the Riemann surface $M$ of $\varepsilon(t)$ is topologically a torus. As in the previous section we use the branch indices 1 and 2 to designate the branches of $\varepsilon(t)$ corresponding to the $-$ and $+$ signs of equation (29), respectively.

The Abelian differential $\varepsilon(t)\,\mathrm{d}t$ is seen to have poles at $0_2$ and $\infty_{1,2}$, and zeros at $0_1$ and the branch points $\pm\sqrt{\alpha}$ and $\pm\sqrt{\beta}$. To find the orders of these zeros and poles and the associated residues we Laurent expand $\varepsilon(t)\,\mathrm{d}t$ around $t = 0$:

$$\varepsilon(t)\,\mathrm{d}t = \left[\frac{1}{2t}(b \mp a\sqrt{\alpha\beta}) + \frac{at}{2}\left\{1 \pm \frac{\sqrt{\alpha\beta}}{2}\left(\frac{1}{\alpha}+\frac{1}{\beta}\right)\right\} + \mathrm{O}(t^3)\right]\mathrm{d}t \tag{31}$$

and around $t = \infty$ (equivalently around $z = 0$, for $z = 1/t$):

$$\varepsilon(t)\,\mathrm{d}t = \left[-\frac{a}{2}(1\mp 1)\frac{1}{z^3} + \left\{-\frac{b}{2} \mp \frac{a(\alpha+\beta)}{4}\right\}\frac{1}{z} \mp \frac{a}{16}(\alpha-\beta)^2 z + \mathrm{O}(z^3)\right]\mathrm{d}z \tag{32}$$

where in both equations (31) and (32) the lower (upper) sign corresponds to branch 1 (2). From the above equations we see that $0_1$ is not a pole but a simple zero, since equation (30) implies $b = a\sqrt{\alpha\beta}$, whereas $0_2$ and $\infty_1$ are both simple poles with residues given by

$$\mathrm{Res}(0_2) = \frac{1}{2}\left(b + a\sqrt{\alpha\beta}\right) = b \tag{33}$$

$$\mathrm{Res}(\infty_1) = -\frac{b}{2} - \frac{a\sqrt{\alpha+\beta}}{4} \tag{34}$$

while $\infty_2$ is a third-order pole with residue given by

$$\mathrm{Res}(\infty_2) = -\frac{b}{2} + \frac{a\sqrt{\alpha+\beta}}{4}. \tag{35}$$

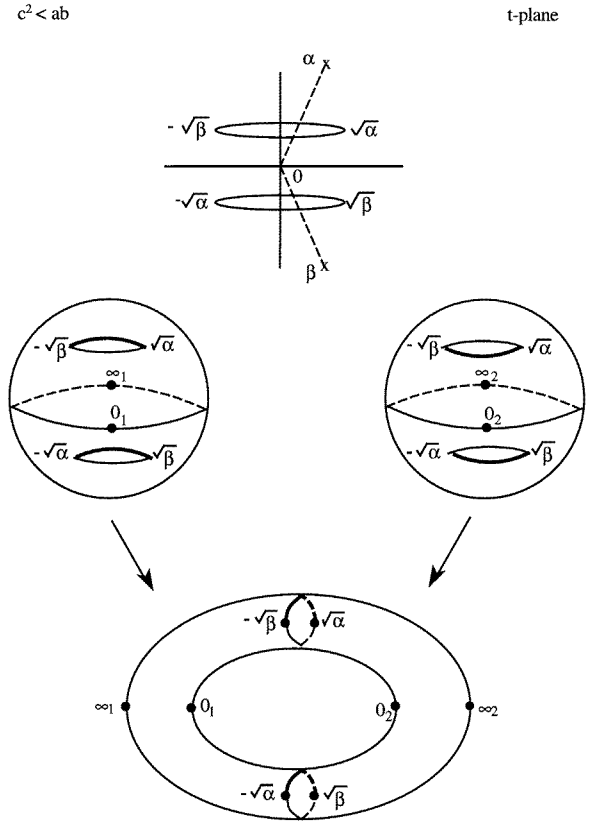


**Figure 4.** The construction of the Riemann surface $M$ of $\varepsilon(t)$ (equation (29)) from cut $t$-planes for (*a*) $c^2 < ab$ and (*b*) $c^2 > ab$. Both cases lead to a torus topologically.

We again note that the sum of the residues vanishes, in agreement with the residue theorem on compact Riemann surfaces. The branch points $\pm\sqrt{\alpha}$ and $\pm\sqrt{\beta}$ are all simple zeros of $\varepsilon(t)\,\mathrm{d}t$. This is due to the fact that, besides $0_1$, $\varepsilon(t)$ does not have any zeros, while $\mathrm{d}t$, as a meromorphic differential on $M$, has simple zeros at $\pm\sqrt{\alpha}$ and $\pm\sqrt{\beta}$.

We also note that $\varepsilon(t)\,\mathrm{d}t$ satisfies the Poincare–Hopf index formula for meromorphic differentials on a compact Riemann surface, which states that the number of zeros (counting multiplicities) minus the number of poles (counting multiplicities) of any meromorphic differential on a compact Riemann surface of genus $g$ is equal to $2g-2$. In the present case $g = 1$, so the number of zeros of $\varepsilon(t)\,\mathrm{d}t$ must be equal to the number of poles of $\varepsilon(t)\,\mathrm{d}t$, being five in each case, counting multiplicities.

Figure 4 illustrates the construction of the Riemann surface $M$ for $\varepsilon(t)$ from the compactified cut Riemann sheets. The location of the branch points $\pm\sqrt{\alpha}$ and $\pm\sqrt{\beta}$ with respect to the real and imaginary $t$-axes depends on the sign of the quantity $c^2 - ab$, which by assumption is non-zero (cf equation (30)). A torus results for both cases.

The topology of the Riemann surface $M$ is closely related to the analytic properties of meromorphic functions and Abelian differentials that can exist on $M$. The relationship is embodied in the Riemann–Roch theorem, which, when applied to the Abelian differential $\omega = \varepsilon(t)\,\mathrm{d}t$ (with $\varepsilon(t)$ specified by equation (29)), implies that $\omega$ belongs to a five-dimensional linear vector space of Abelian differentials on $M$ with poles of orders not

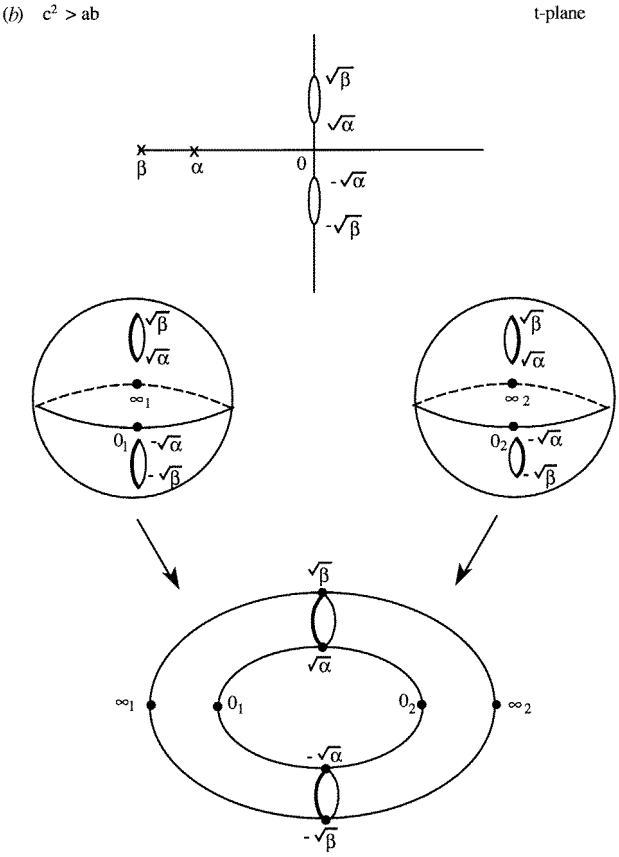


**Figure 4.** (Continued)

greater than those of $\omega$ at the same points†.

Since $\Pi_1(M) = H_1(M) = \mathbb{Z}^2$ for a torus, the homology (homotopy) class index $\mu$ in equation (17) labels two integers $n \in \mathbb{Z}$ and $m \in \mathbb{Z}$. We will pick specific oriented closed curves $\zeta$ and $\eta$ belonging to the classes $(1, 0)$ and $(0, 1)$ which do not traverse any of the singularities of $\varepsilon(t)\,\mathrm{d}t$, as in figure 5. Then an arbitrary curve $\mathcal{C}_\mu$ from $\tau_1$ to $\tau_2$ (where $\tau_1$ is some real $t$-value on the first sheet of $\varepsilon(t)$ and $\tau_2$ the corresponding real value on the second sheet) is homotopic to $I_0 + (n \text{ loops of } \zeta) + (m \text{ loops of } \eta)$, where $I_0$ is a direct path from $\tau_1$ to $\tau_2$ not traversing any singularities of $\varepsilon(t)\,\mathrm{d}t$. We write

$$\mathcal{C}_\mu \sim I_0 \zeta^n \eta^m. \tag{36}$$

Note that $\tau_1 \neq 0$ and $\tau_2 \neq 0$ are chosen as the end points of $\mathcal{C}_\mu$ due to the fact that $0_2$ is a pole of $\omega$. This choice has no effect on the transition amplitude given by equation (17).

† This result is obtained by considering the divisor

$$D = -0_2 - \infty_1 - 3\infty_2$$

in the Riemann–Roch theorem, where $0_2$, $\infty_1$, and $\infty_2$ are poles of orders 1, 1, and 3, respectively, of the Abelian differential $\varepsilon(t)\,\mathrm{d}t$ ($\varepsilon d(t)$ given by equation (29)). The Riemann–Roch theorem, a deep result relating the topological and analytical properties of compact Riemann surfaces, is discussed in any standard work on Riemann surfaces, algebraic curves, and algebraic geometry, such as [15, 16, 19].

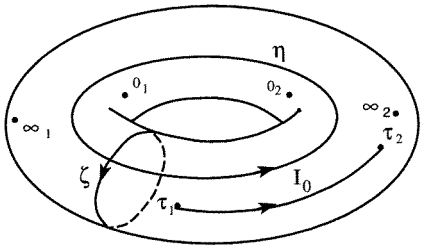


**Figure 5.** Non-trivial oriented homotopy paths $\zeta$ and $\eta$ on the Riemann surface of $\varepsilon(t)$ (equation (29)). A general path from $\tau_1$ to $\tau_2$ leading to quantum transition is homotopic to $I_0\zeta^n\eta^m$, where $n, m \in \mathbb{Z}$.

Based on a general theorem of Abelian integrals on a Riemann surface, the transition amplitude $C_2(\infty)$ given by equation (17) can then be written in the form [20]

$$C_2(\infty) = \sum_{\substack{n,m,\\ k_1,k_2,k_3}}{}' \exp\{\mathrm{i}(n\gamma_\zeta + m\gamma_\eta)\} \exp\left[ -\frac{\mathrm{i}}{\hbar}\left\{ \int_{I_0} \varepsilon(t)\,\mathrm{d}t + n\int_\zeta \varepsilon(t)\,\mathrm{d}t \right.\right.$$
$$\left.\left. + m\int_\eta \varepsilon(t)\,\mathrm{d}t + 2\pi\mathrm{i}(k_1\,\mathrm{Res}(0_2) + k_2\,\mathrm{Res}(\infty_1) + k_3\,\mathrm{Res}(\infty_2)) \right\}\right]. \tag{37}$$

In this equation $n$, $m$, $k_1$, $k_2$, $k_3$ all $\in \mathbb{Z}$, the three residues are given by equations (33)–(35), $\gamma_\zeta$ and $\gamma_\eta$ are the geometric phases corresponding to the closed loops $\zeta$ and $\eta$, respectively (cf equations (9) and (17)) and the prime above the summation sign denotes a restricted sum: only those values of $n$, $m$, $k_1$, $k_2$, $k_3$ are allowed such that the quantity within the brackets $\{\}$ has a negative imaginary part. We note that $\zeta$ and $\eta$ are specific closed loops on $M$, not homotopy classes.

For the remainder of this section we will study the relationships between the three integrals occurring in equation (37).

First we display in figure 6 a possible choice for the path $I_0$ on the cut Riemann spheres corresponding to the two sheets of $\varepsilon(t)$ for both the cases $c^2 < ab$ and $c^2 > ab$ (cf figure 4). In each case $I_0'$ represents the complex-conjugated path of $I_0$. It is clear we can choose the loop $\eta$ (of figure 5) such that it is the combination of $I_0$ and $-I_0'$. Also, since $\varepsilon(t)$ is real on the real axis, the reflection principle implies that

$$\int_{I_0} \varepsilon(t)\,\mathrm{d}t = \left( \int_{I_0'} \varepsilon(t)\,\mathrm{d}t \right)^*. \tag{38}$$

Thus

$$\int_\eta \varepsilon(t)\,\mathrm{d}t = \int_{I_0} \varepsilon(t)\,\mathrm{d}t - \int_{I_0'} \varepsilon(t)\,\mathrm{d}t = 2\mathrm{i}\,\mathrm{Im}\int_{I_0} \varepsilon(t)\,\mathrm{d}t. \tag{39}$$

To relate $\int_\zeta \varepsilon(t)\,\mathrm{d}t$ to $\int_\eta \varepsilon(t)\,\mathrm{d}t$ we use the following Riemann bilinear relation on two closed differentials $\theta$ and $\tilde{\theta}$ on a compact Riemann surface $M$ of genus $g$†:

$$\int_{\partial M} f\tilde{\theta} = \sum_{l=1}^{g}\left[ \int_{\zeta_l} \theta \int_{\eta_l} \tilde{\theta} - \int_{\eta_l} \theta \int_{\zeta_l} \tilde{\theta} \right] \tag{40}$$

where $\theta = \mathrm{d}f$, $\partial M$ is the boundary of a $4g$-sided polygon representing the canonically dissected Riemann surface with oriented sides $\zeta_l$, $\eta_l$, $\zeta_l^{-1}$, $\eta_l^{-1}$ which generate $\Pi_1(M)$. For

† See, for example, section III.3 of [15].

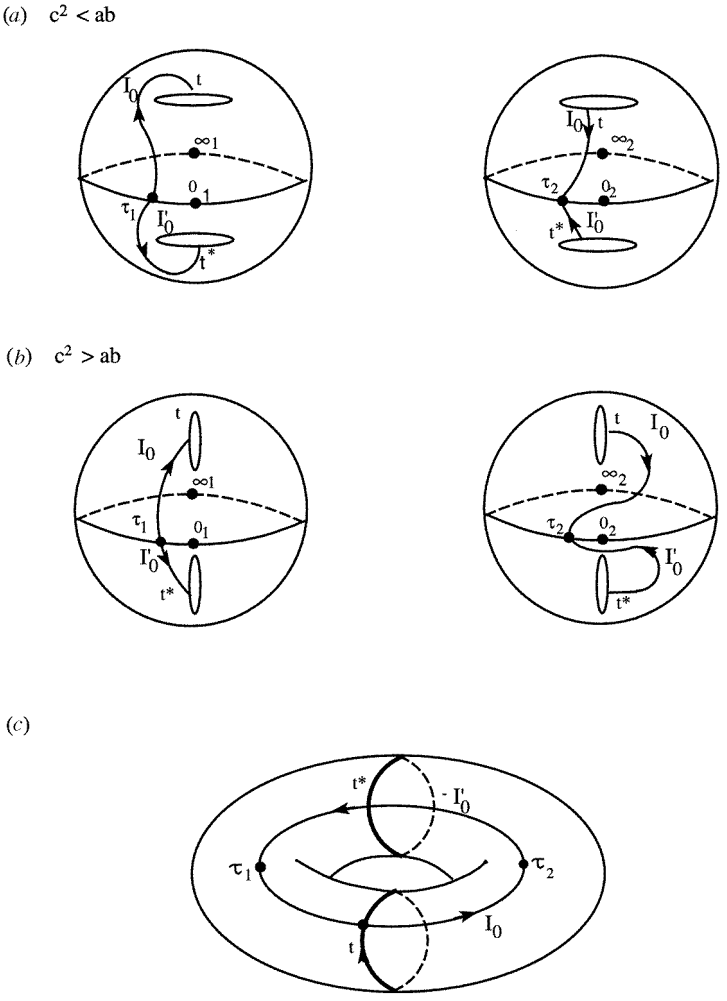


**Figure 6.** A choice of the path $I_0$ in equation (37) and figure 5 for the two cases (*a*) $c^2 < ab$ and (*b*) $c^2 > ab$, displayed on cut Riemann spheres; (*c*) represents both cases (*a*) and (*b*) on the Riemann surface $M$ (a torus). $t$ and $t^*$ (complex conjugate of $t$) represent distinct points on the cut-edges and thus distinct points on $M$. $I_0'$ is the complex conjugate of $I_0$.

the present case $g = 1$, so this polygon is simply a rectangle with opposite sides identified. We choose $\theta$ to be the holomorphic differential

$$\theta = \mathrm{d}f \equiv \frac{\mathrm{d}t}{\sqrt{(t-\sqrt{\alpha})(t+\sqrt{\alpha})(t-\sqrt{\beta})(t+\sqrt{\beta})}} \tag{41}$$

where $\alpha$ and $\beta$ are given by equation (30) and $\tilde{\theta}$ to be the Abelian action differential

$$\tilde{\theta} \equiv \varepsilon(t)\,\mathrm{d}t. \tag{42}$$

Then

$$\int_{\partial M} f(t)\varepsilon(t)\,\mathrm{d}t = \Omega_\zeta \int_\eta \varepsilon(t)\,\mathrm{d}t - \Omega_\eta \int_\zeta \varepsilon(t)\,\mathrm{d}t \tag{43}$$

where

$$\Omega_\zeta \equiv \int_\zeta \frac{\mathrm{d}t}{\sqrt{\left(t-\sqrt{\alpha}\right)\left(t+\sqrt{\alpha}\right)\left(t-\sqrt{\beta}\right)\left(t+\sqrt{\beta}\right)}} \tag{44}$$

and

$$\Omega_\eta \equiv \int_\eta \frac{\mathrm{d}t}{\sqrt{\left(t-\sqrt{\alpha}\right)\left(t+\sqrt{\alpha}\right)\left(t-\sqrt{\beta}\right)\left(t+\sqrt{\beta}\right)}} \tag{45}$$

are recognized to be the two basic periods of the (doubly periodic) elliptic function defined as the inverse function, $t(w)$, of

$$f(t) = \int_{t_0}^{t} \frac{\mathrm{d}t}{\sqrt{(t^2-\alpha)(t^2-\beta)}} \tag{46}$$

where $t_0$ is an arbitrary point in $M$†. Choosing $t_0 = \sqrt{\alpha}$, we immediately see that

$$f(0_1) + f(0_2) = f(\infty_1) + f(\infty_2) = 0 \tag{47}$$

due to the sign difference of the square root in the integrand of equation (46) on the different Riemann sheets.

The left-hand side of equation (43) can be evaluated by the residue theorem:

$$\begin{aligned}\int_{\partial M} f(t)\varepsilon(t)\,\mathrm{d}t &= -2\pi\mathrm{i}a\left[\frac{\sqrt{\alpha\beta}}{2}\{f(0_1)-f(0_2)\}+\left(\frac{\alpha+\beta}{4}\right)\{f(\infty_1)-f(\infty_2)\}\right] \\ &= -2\pi\mathrm{i}aA\left[\sqrt{\alpha\beta}+\left(\frac{\alpha+\beta}{2}\right)\right]\end{aligned} \tag{48}$$

where

$$A \equiv f(0_1) = -f(0_2) = \tfrac{1}{2}\{f(0_1)-f(0_2)\}. \tag{49}$$

In the second equality of equation (48), we have used the following fact:

$$f(\infty_1) - f(\infty_2) = f(0_1) - f(0_2) = 2A \tag{50}$$

which follows from applying Canchy's theorem to the closed loop shown in figure 7(*a*). Figure 7(*b*) displays the values of $\int \mathrm{d}f$ over segments of the homotopy loop $\eta$ in terms of the constant $A$ defined in equation (49), obtained by application of the reflection principle and the fact that $f$ has opposite signs on the two Riemann sheets comprising $M$. This figure also shows that

$$\Omega_\eta = 2\mathrm{i}\,\mathrm{Im}\,A \tag{51}$$

which implies that the basic period $\Omega_\eta$ is purely imaginary.

At this point we have to distinguish between the two cases (i) $c^2 > ab$ (figure 4(*b*)) and (ii) $c^2 < ab$ (figure 4(*a*)). In case (i) it is easily seen, by referring the contour of integration in equation (46) (with $t_0 = \sqrt{\alpha}$ and $t = 0_1$) to figure 4(*b*), that $A = f(0_1)$ is purely imaginary. Thus equation (51) implies

$$\Omega_\eta = 2A \qquad (c^2 > ab). \tag{52}$$

We then obtain, from equations (43) and (48), the following relationship between $\int_\zeta \varepsilon(t)\,\mathrm{d}t$ and $\int_\eta \varepsilon(t)\,\mathrm{d}t$ for the case $c^2 > ab$:

$$\int_\zeta \varepsilon(t)\,\mathrm{d}t = \frac{1}{\tau}\int_\eta \varepsilon(t)\,\mathrm{d}t + \mathrm{i}\pi a\left[\sqrt{\alpha\beta}+\left(\frac{\alpha+\beta}{2}\right)\right] \qquad (c^2 > ab) \tag{53}$$

† See, for example, ch 1 of [17].

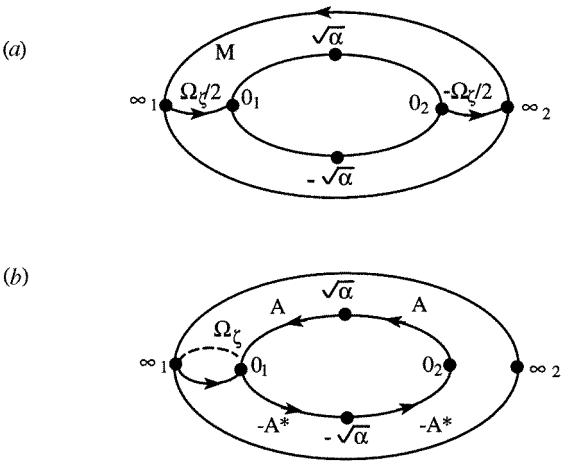


**Figure 7.** Integration paths and values of the integrals for the holomorphic differential $\mathrm{d}f$ defined by equation (41). $\Omega_\zeta$ is a basic period of the elliptic function defined by $\mathrm{d}f$ (equation (44)) and $A$ is defined by equation (49).

where

$$\tau \equiv \frac{\Omega_\eta}{\Omega_\zeta}. \tag{54}$$

We recall from equation (39) that $\int_\eta \varepsilon(t)\,\mathrm{d}t$ is purely imaginary.

For case (ii): $c^2 < ab$, $A$ is no longer purely imaginary. We have

$$2A = f(0_1) - f(0_2) = \int_{C_1+C_2+C_3} \mathrm{d}f \tag{55}$$

where the contours $C_1, C_2, C_3$ on the two cut Riemann sheets and their complex conjugate counterparts on the lower half planes, $C_4, C_5, C_6$, are shown in figure 8. Defining

$$\int_{C_1} \mathrm{d}f \equiv A' \tag{56}$$

$$\int_{C_2} \mathrm{d}f \equiv B \tag{57}$$

the opposite signs of the two branches of the integrand and the reflection principle imply

$$\int_{C_3} \mathrm{d}f = A' \tag{58}$$

$$\int_{C_4} \mathrm{d}f = -A'^* \tag{59}$$

$$\int_{C_5} \mathrm{d}f = -B^* \tag{60}$$

$$\int_{C_6} \mathrm{d}f = -A'^*. \tag{61}$$

Figure 7(*b*) and figure 8 then show that

$$\Omega_\eta = \mathrm{i}(2\,\mathrm{Im}\,A' + \mathrm{Im}\,B) \qquad (c^2 < ab). \tag{62}$$

Now refer to the contour $C$ on the first cut Riemann sheet in figure 8($c$). Since $\mathrm{d}f$ is holomorphic, $\int_c \mathrm{d}f = 0$. It is easily seen from equation (41) that the integral along the infinite quarter-circle vanishes, while the integral along the negative real axis equals $\Omega_\zeta/2$ (figure 7($a$)). These results, together with the facts that the integral along the positive imaginary axis is purely imaginary and that $\Omega_\zeta$ is real, imply

$$\mathrm{Re}\, B = \Omega_\zeta/2. \tag{63}$$

Equation (55) thus yields

$$f(0_1) - f(0_2) = 2A' + B = \Omega_\eta + \Omega_\zeta/2. \tag{64}$$

Analogous to equation (50) we have

$$f(\infty_1) - f(\infty_2) = f(0_1) - f(0_2) = \Omega_\eta + \Omega_\zeta/2. \tag{65}$$

Finally equations (43) and (48) lead to the following relationship between $\int_\zeta \varepsilon(t)\,\mathrm{d}t$ and $\int_\eta \varepsilon(t)\,\mathrm{d}t$ for the case $c^2 < ab$:

$$\int_\zeta \varepsilon(t)\,\mathrm{d}t = \frac{1}{\tau}\int_\eta \varepsilon(t)\,\mathrm{d}t + \mathrm{i}\pi a\left(1 + \frac{1}{2\tau}\right)\left\{\sqrt{\alpha\beta} + \frac{(\alpha+\beta)}{2}\right\} \qquad (c^2 < ab) \tag{66}$$

where $\tau$ is defined by equation (54).

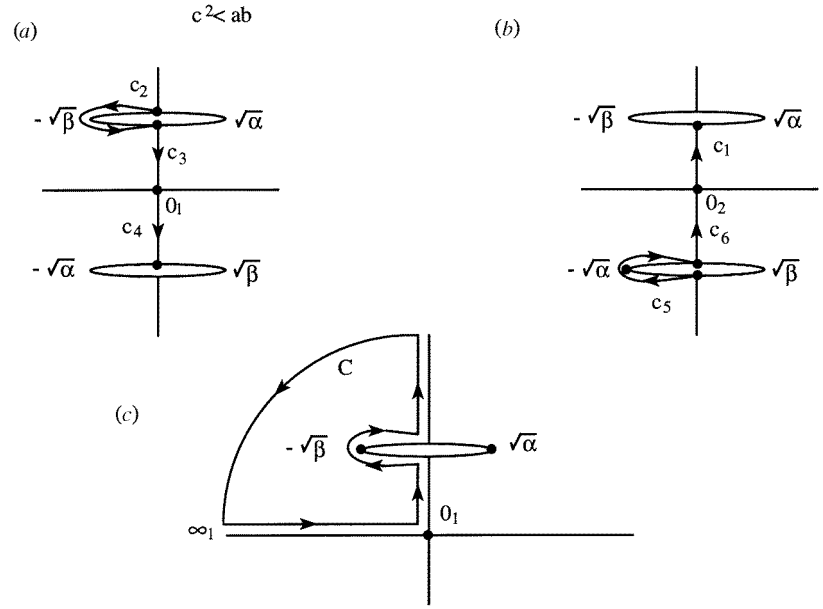


**Figure 8.** ($a$) and ($b$) represent contours of integration (in equations (55)–(61)) displayed on the cut Riemann sheets of the holomorphic differential $\mathrm{d}f$ (equation (41)). ($c$) represents a contour on the first sheet to establish equation (63). The entire figure applies only to the case $c^2 < ab$.

The above analysis shows that the Abelian integrals in our central result of this section (equation (37) for the transition amplitude) all depend on just one integral $\int_{I_0} \varepsilon(t)\,\mathrm{d}t$ (recall equation (39)) and the ratio of the two basic periods, $\tau$, of the elliptic function defined by equation (46).

## 6. Directions for further study

In this paper we hope to have conveyed some of the utility and elegance of the mathematics of algebraic functions and Abelian integrals on compact Riemann surfaces as applied to the semiclassical theory of molecular collisions. We illustrated the mathematical ideas and techniques involved by two simple models, possibly the simplest ones for the genus zero and genus one cases. The $g = 0$ model leads to the tried-and true Landau–Zener formula. The success of our approach in this simple but important case motivates the study of models with more complicated topology and complex structures. Although it is not immediately clear how our $g = 1$ model relates to specific molecular systems, we hope it gives some flavour of the problems one is likely to encounter in more realistic models of molecular collisions, which will most likely involve $g > 1$ compact Riemann surfaces, or indeed non-compact ones. In particular it is quite instructive to see how differences in the Hamiltonian matrices for these models can lead to basic differences in the topological and analytic structures of the Riemann surfaces governing quantum transitions. The $g > 1$ cases, however, will require considerably more sophisticated mathematical tools as the uniformization of the corresponding algebraic curves require more complicated meromorphic function fields than the elliptic functions encountered in the last section.

There is a degree of magic to the Landau–Zener formula, which owes its power perhaps to the very simplicity of the model on which it is based. The Hamiltonian for this model (equation (18)) only describes the physical situation locally (near the transition region in the nuclear coordinates). Yet as we have amply demonstrated in this paper, it is the very global properties (topological and analytic) of the Riemann surface of the potential energy function $\varepsilon(t)$ that dictate the (physically) local quantum transitions. Indeed, the transition amplitudes for transitions which occur physically near $t = 0$ curiously depend solely on the residues of $\varepsilon(t)\,\mathrm{d}t$ at $t = \infty$. A similar state of affairs exists in the $g = 1$ model. Now, in a physical sense, what happens around $t = \infty$ in a more realistic model (with very likely large $g$) will differ markedly from the low genus models. The question thus arises: To what extent can one approximate $H(t)$ in equation (1) locally but make use of the global properties of the approximated form to calculate transition probabilities? This intriguing question definitely merits further investigation.

Another important problem that is not fully addressed in this paper is the proper choice of meromorphic functions $R_i(t)$ representing classical trajectories for the nuclear coordinates. These functions allow us to work with an algebraic curve (defined by equation (4)) relating $\varepsilon$ to $t$ rather than an algebraic variety (relating $\varepsilon$ to $R_1, \ldots, R_m$)—a considerably more complicated mathematical object. A reasonable procedure is to obtain the $R_i(t)$ from integration of Hamilton's equations using the single potential function $\varepsilon_k(R_1, \ldots, R_m)$ (the branch of the potential function $\varepsilon(R_1, \ldots, R_m)$ defined from the above-mentioned variety) corresponding to the initial electronic state. This approach, however, leaves open the problem of the possibility of transitions from state $k$ to state $l (k \neq l)$ within some interval of time. Another procedure is to incorporate local transitions within the framework of Hamilton's equations by complexifying $dt$ at some appropriate (real) time instant to bring about instantaneous potential-energy surface 'hops'. This procedure also suffers from serious mathematical difficulties and physical ambiguities, such as the problem of the continuity of the canonical momenta at the instant of transition and the choice of the exact instant of transition. The most practical approach seems to be the search for empirical choices for local nuclear trajectories $R_i(t)$ (in the spirit of the Landau–Zener straight-line trajectories), short of pursuing a rigorous classical mechanical analysis, which will lead to acceptable approximations to particular systems.

A final problem deserving a more complete treatment is the geometric phase factor (equation (7)). These have not been calculated explicitly for the $g = 1$ model. A more thorough investigation would involve studying the analytic properties of $\phi(t)$ and $\dot{\phi}(t)$ considered as analytic continuations of $\phi_i(t)$ from the real $t$-axis and possibly looking into the gauge theory aspects of $\langle\phi|\dot{\phi}\rangle$ considered as connections on vector bundles on Riemann surfaces.

## Acknowledgment

The author is grateful for helpful discussions with M Nakashima, who clarified several points on the mathematics of the paper.

## References

[1] See, for example, Child M S (ed) 1979 *Semiclassical Methods in Molecular Scattering and Spectroscopy, NATO Advanced Study Institutes Series C* (Boston: D Reidel)
[2] Pechukas P 1969 *Phys. Rev.* **181** 166; 1969 **181** 174
[3] Miller W H 1974 *Adv. Chem. Phys.* **25** 69
[4] Miller W H and George T F 1972 *J. Chem. Phys.* **56** 5637; 1972 **56** 5668
[5] See, for example, Schulman L S 1981 *Techniques and Applications of Path Integration* (New York: Wiley)
[6] Gutzwiller M C 1990 *Chaos in Classical and Quantum Mechanics* IAM vol 1 (New York: Springer)
[7] Berry M V 1984 *Proc. R. Soc.* A **392** 45 (also reproduced in [8])
[8] Shapere A and Wilczek F (ed) 1989 *Geometric Phases in Physics (Advanced Series in Mathematical Physics)* vol 5 (Singapore: World Scientific)
[9] Nakahara M 1990 *Geometry, Topology and Physics, Graduate Student Series in Physics* (New York: Adam Hilger)
Schlichenmaier M 1989 *An Introduction to Riemann Surfaces, Algebraic Curves and Modular Spaces (Lecture Notes in Physics)* vol 322 (Berlin: Springer)
[10] Landau L D and Lifshitz E M 1977 *Quantum Mechanics* section 52 (Oxford: Pergamon)
Landau L D 1932 *Phys. Z. Sowjet.* **1** 88; 1932 **2** 46 (Engl. Transl. 1967 *Collected Papers of L D Landau* ed D ter Haar (New York: Gordon and Breach))
[11] Zener A 1932 *Proc. R. Soc.* A **137** 696
[12] Dykhne A M 1962 *Sov. Phys.–JETP* **14** 941
[13] Hwang J-T and Pechukas P 1977 *J. Chem. Phys.* **67** 4640
[14] Moody J, Shapere A and Wilczek F 1989 *Adiabatic Effective Lagrangians* p 160 ref [8]
[15] See, for example, Farkas H M and Kra I 1992 *Riemann Surfaces, Graduate Texts in Math* (New York: Springer)
[16] See, for example, Griffiths P A 1989 *Introduction to Algebraic Curves, AMS (Translations of Mathematical Monographs, 76)* (Providence, RI: AMS); and also section III.4 of [15]
[17] For relatively non-technical discussions of algebraic functions, see Siegel C L 1969 *Topics in Complex Function Theorey vol I: Elliptic Functions and Unformation Theory* section 2.1 (New York: Wiley)
Jones G A and Singerman D 1987 *Complex Functions: an Algebraic and Geometric Viewpoint* section 4.14 (Cambridge: Cambridge University Press)
[18] Berry M V 1984 *J. Phys. A: Math. Gen.* **17** 1225
[19] For a relatively non-technical discussion of Abelian integrals, see Siegel C L 1971 *Topics in Complex Function Theory vol II: Automorphic Functions and Abelian Integrals* ch 4 (New York: Wiley)
[20] See, for example, Bliss G A 1966 *Algebraic Functions* (New York: Dover) p 97